Available online at www.sciencedirect.com
SCIENCE DIRECT®
Journal of Solid State Chemistry 178 (2005) 3426–3430
JOURNAL OF SOLID STATE CHEMISTRY
www.elsevier.com/locate/jssc

# The role of Mn in the electronic structure of $Ba_3Ti_2MnO_9$

G. Radtke[a], C. Maunders[b], S. Lazar[c], F.M.F. de Groot[d], J. Etheridge[b], G.A. Botton[a,c,*]

[a]*Brockhouse Institute for Materials Research, McMaster University, Hamilton, Canada*
[b]*School of Physics and Materials Engineering, Monash University, Victoria, Australia*
[c]*National Centre for HREM, Kavli Institute of Nanoscience, Delft University of Technology, Delft, The Netherlands*
[d]*Department of Inorganic Chemistry and Catalysis, Utrecht University, Utrecht, The Netherlands*

Received 19 July 2005; accepted 28 August 2005
Available online 29 September 2005

**Abstract**

The energy loss near edge structure (ELNES) of the O–K, Ti–$L_{23}$ and Mn–$L_{23}$ edges have been recorded in hexagonal $Ba_3Ti_2MnO_9$ with an energy resolution of 0.10–0.20 eV using a monochromator on a commercial transmission electron microscope (TEM) and compared with a tetragonal $BaTiO_3$ reference sample. The formal valency and symmetry of Mn have been determined using atomic multiplets calculations and its effect on the electronic structure of $BaTiO_3$ has been interpreted through a molecular-orbital model.


*Keywords:* Energy loss near edge fine structure; Transition metal oxide; Hexagonal perovskite; Electronic structure

## 1. Introduction

Electron energy loss spectroscopy (EELS) in the transmission electron microscope (TEM) is one of the most powerful solid-state spectroscopies mainly because of its high spatial [1,2] and energy [3,4] resolutions. In particular, the energy loss near edge structure (ELNES), probing the site- and symmetry-projected density of unoccupied states [5], are widely used to investigate the electronic structure of materials. Its high sensitivity to the nature of chemical bonds and to the local coordination around the excited atom is crucial to understand the relationship between the local electronic structure and the physical properties of materials. The recent development of monochromators and high-energy resolution spectrometers on commercial instruments has pushed the energy resolution toward the limit of 0.1–0.2 eV. This major advance allows the acquisition of ELNES with a negligible contribution from experimental broadening which is now of order or smaller than the broadening due to the finite lifetime of initial and final states for the most commonly studied edges in solids. These experimental spectra are, therefore, equivalent to those obtained in X-ray absorption spectroscopy (XAS).

Doping of $BaTiO_3$ with transition metals such as Mn leads to important modifications of its physical properties. For example, an effective method for the stabilisation of the high temperature hexagonal phase of $BaTiO_3$ at room temperature is by the substitution of Ti with M = V, Cr, Mn, Fe, Co, Ru, Rh, Ir, or Pt with the stoichiometry $Ba_3Ti_2MO_9$ [6]. The M atoms occupy a Ti 4-fold site in each of the two $Ti_2O_9$ co-ordination groups and the $Ti_2O_9$ groups are linked by corner sharing $TiO_6$ octahedra. The close approach and repulsion of the Ti atoms in the $Ti_2O_9$ group results in a destabilisation of hexagonal $BaTiO_3$ as it is cooled to room temperature. It has thus been postulated that M substitution allows the overlap of M-Ti *d*-orbitals which acts as the stabilising mechanism [6–10]. It has also been shown that the presence oxygen vacancies at the interface of the $Ti_2O_9$ group may contribute to the stabilisation [11]. The goal of this paper is to understand the effect of Mn on the electronic structure of $BaTiO_3$ through a study of the core loss spectra recorded in $Ba_3Ti_2MnO_9$ and in a reference sample of tetragonal $BaTiO_3$. Recent structural studies have uncovered the

*Corresponding author. Brockhouse Institute for Materials Research, McMaster University, 1280 Main Street West (ABB 429), Hamilton, Ont., Canada L8S 4M1. Fax: +1 905 521 2773.
*E-mail address:* gbotton@mcmaster.ca (G.A. Botton).

0022-4596/$ - see front matter © 2005 Elsevier Inc. All rights reserved.
doi:10.1016/j.jssc.2005.08.020

Mn/Ti ordering in $Ba_3Ti_2MnO_9$, and investigations of its electrical properties due to the presence of Mn, acting as an effective acceptor dopant have been performed [12]. However, to our knowledge, no detailed investigation of the influence of Mn on the electronic structure of $BaTiO_3$ has been reported so far. The experimental data are analysed and interpreted with the help of ligand field multiplets and molecular orbital calculations.

## 2. Material and methods

The experimental spectra have been recorded on a FEI Tecnai 200 FEG microscope equipped with a monochromator and a high-resolution energy loss spectrometer. This system enables the recording of EELS spectra with an energy resolution of 0.10–0.20 eV (measured at full width at half maximum (FWHM) of the zero loss peak), as described elsewhere [4]. In these experiments, the probe size was a few tens of nm. The spectra were acquired in diffraction mode with a large collection angle ($>10$ mrad) and a dispersion of 0.05 eV/channel. For each edge shown hereafter, a series of spectra recorded with relatively short acquisition times (between 5 and 30 s) were added yielding to a total acquisition time varying between 50 and 300 s. The background, modelled with a power law, has been fitted on the pre-edge region, extrapolated and finally extracted using standard procedures. We ensured that the samples were thin enough to consider multiple inelastic scattering contributions as negligibles. The TEM samples were prepared by crushing the powder in ethanol and by dispersing the suspension on a holey carbon-covered Cu grid.

## 3. Results

### 3.1. Ti–$L_{23}$ edge

The Ti–$L_{23}$ edge in $Ba_3Ti_2MnO_9$ is displayed in Fig. 1. The shape of this edge is characteristic of a $d^0$ transition metal in octahedral symmetry [13]. In the one electron picture, the four preeminent lines can be interpreted in a simple way: the $2p$ spin–orbit coupling gives rise to two strong lines separated by a value of $\frac{3}{2}\times\zeta_{2p}$ ($\zeta_{2p}$ is the radial part of the spin-orbit matrix element), respectively (the $L_3$ and $L_2$ edges), which in turn are split in two lines by the octahedral crystal field. The main effect of the crystal field is indeed to split the $3d$ (final) states in two levels of $t_{2g}$ and $e_g$ symmetries, respectively. However, this approach usually fails to describe the fine structure observed near transition metal $L_{23}$ edges. A quantitative description of these edges requires an explicit treatment of electron–electron interactions and ligand field multiplets calculations [14]. In the same figure we show the experimental Ti–$L_{23}$ edge acquired in a sample of $BaTiO_3$ as a reference for $Ti^{4+}$, in $Ba_2TiNbO_6$ as a reference for $Ti^{3+}$ and the theoretical $L_{23}$ edge of $Ti^{4+}$ calculated in an octahedral crystal field with a 10 Dq parameter of 1.80 eV (see Table 1). The four preeminent lines being well separated, it is possible to use specific Lorentzian broadenings for each of them. We applied here the approach developed by de Groot et al. in Ref. [13] separating the contributions of Coster–Kronig Auger and solid-state broadenings. The best agreement is achieved using the same values as found for the Ti–$L_{23}$ edge in the parent compound $FeTiO_3$ in Ref. [13]. From the important similarities with the reference spectrum recorded in $BaTiO_3$ and the excellent overall agreement with the theoretical spectrum, it can be deduced that the Ti is still tetravalent in $Ba_3Ti_2MnO_9$. In particular, the presence of a non-negligible amount of trivalent Ti would result in a substantial modification of the fine structure, as predicted from the multiplets calculations [15] or observed experimentally [16,17] in mixed valence compounds. This strong modification of the fine structure associated with a reduction of the formal valency of the Ti is illustrated in the case of the reference compound $Ba_2TiNbO_6$. However, a previous study [18] of the Ti–$L_{23}$ edge pointed out that a minor concentration of $Ti^{3+}$ in

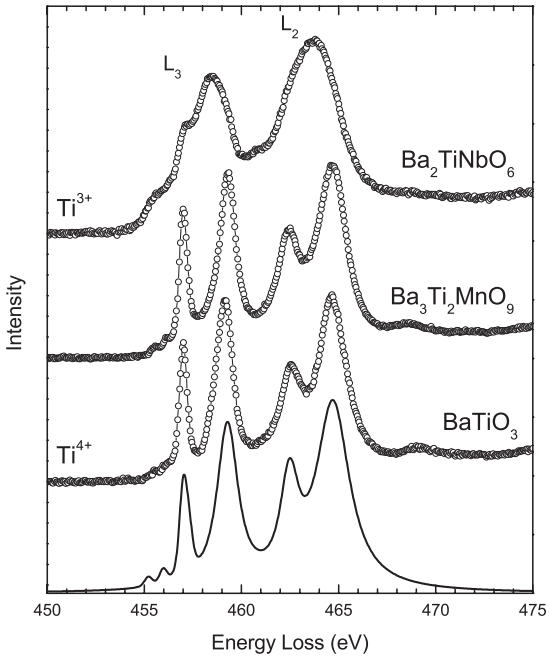


Fig. 1. A comparison between the experimental Ti–$L_{23}$ edge in $BaTiO_3$, $Ba_2TiNbO_6$ and $Ba_3Ti_2MnO_9$ (circles) and the ligand field multiplets calculations of $Ti^{4+}$ in octahedral crystal field (solid line).

Table 1
Parameters used in the ligand field multiplets calculations of Ti and Mn–$L_{23}$ edges

| | $\kappa_{pd}$ (%) | $\kappa_{dd}$ (%) | 10 Dq (eV) |
|---|---|---|---|
| $Ti^{4+}$ | 100 | — | 1.80 |
| $Mn^{4+}$ | 60 | 45 | 2.05 |

The scaling factors used for the Slater integrals are given in percentage of the atomic values.

minerals containing both valences is not easily detectable. If this edge cannot be considered as a proof of the *absence* of trivalent Ti, it leads to the reasonable conclusion that *if* trivalent Ti is present, its concentration is negligible. The high-lying structures visible on the experimental spectra at around 468–469 eV are not reproduced by this single configuration calculation and thus should be addressed. The nature of these features is still not clear and has been interpreted as charge transfer [19] or polaronic satellites [20]. The main information resulting from the analysis of this edge is that the Ti environment is not strongly modified by the presence of Mn with respect to the case of $BaTiO_3$ and that no change of the Ti formal valency or a strong distortion of the O octahedra can be detected. In particular, the presence of oxygen vacancies, leading to a $Ti^{4+}$ to $Ti^{3+}$ reduction in $BaTiO_{3-\delta}$ [21] or $SrTiO_{3-\delta}$ [22] and then to an important change of the fine structure is not observed.

### 3.2. Mn–$L_{23}$ edge

The Mn–$L_{23}$ edge has been recorded and is shown in Fig. 2. In order to keep electrical neutrality in the unit cell, the Mn is predicted to be tetravalent. However, the experimental edge does not agree with the theoretical ionic calculations of $Mn^{4+}$ in octahedral symmetry [15]. This deviation from ionic calculations can be attributed to a non-negligible hybridisation of the transition metal with the ligand atoms. These effects can be included in the multiplets calculations by a reduction of the Slater integrals from their atomic values [23]. Different reduction factors are usually used for the integrals describing the 3*d*–3*d* and 2*p*–3*d* interactions, $\kappa_{dd}$ and $\kappa_{pd}$, respectively. This difference is justified by the fact that the 2*p* core-states are not affected by the hybridisation. These parameters together with the crystal field strength 10 Dq have been optimised so as to get the best agreement with the experimental spectrum. Their values are given in Table 1 and the corresponding spectrum is displayed on Fig. 2. In this case, a Lorentzian broadening of 0.1 eV for the $L_3$ edge and 0.3 eV for the $L_2$ edge have been used in addition to the 0.2 eV Gaussian experimental broadening. The over all agreement between theoretical and experimental spectra is good even if the detailed fine structure of the $L_3$ edge is not exactly reproduced. However, the similarities of this experimental spectrum with X-ray absorption $L_{23}$ edges of $Mn^{4+}$ in complex molecules [24] and in solids such as $Li_2MnO_3$ [25], $MnO_2$ [26] or minerals [27], strengthen our belief that Mn is in the 4+ oxidation state. Such a strong reduction of the Slater integrals reveals the fact that the Mn ground state cannot be described with only a $|3d^3\rangle$ ionic configuration but as a mixture of $|3d^3\rangle$ and $|3d^4\,\underline{L}\rangle$ configurationswhere $\underline{L}$ denotes a ligand-hole (here an O-2*p* hole) with a non-negligible weight of the second configuration. To summarize these results, the ligand field multiplets calculations allow us to assume a $^4A_2$ symmetry of the $Mn^{4+}$ atom in octahedral site but also reveal a covalent character of the Mn–O bonding.

### 3.3. O–K edge

Complementary information on the role of Mn in the bonding of this compound can be obtained from the O–K edge. This edge is displayed in Fig. 3 together with the O–K edge acquired in a $BaTiO_3$ reference sample. Contrary to transition metal $L_{23}$ edges where the multiplets effects are dominant, K edges can be interpreted in terms of the electronic structure of the compounds under investigation [5,28]. In $BaTiO_3$ as in other $d^0$ perovskites [29,30], the bottom of the conduction band is dominated by the empty Ti-3*d* states split in the $t_{2g}$ and $e_g$ sub-bands under the octahedral crystal field. The weak $\pi$ hybridisation of

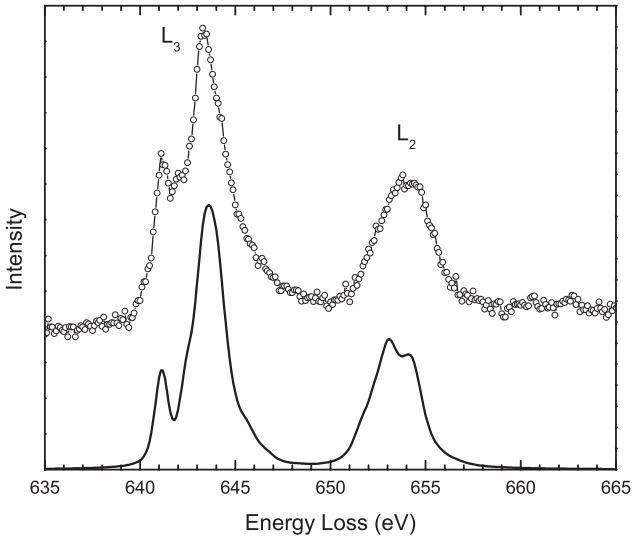


Fig. 2. A comparison between the experimental Mn–$L_{23}$ edge (circles) and the ligand field multiplets calculations of $Mn^{4+}$ in octahedral crystal field with covalency included (solid line) .

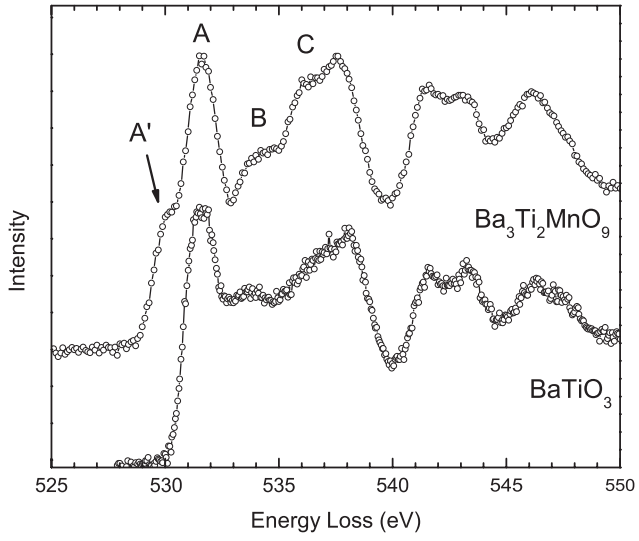


Fig. 3. A comparison between the experimental O–K edges in $BaTiO_3$ and $Ba_3Ti_2MnO_9$.

the Ti-3*d* $t_{2g}$ with O-2*p* orbitals leads to the formation of a narrow band corresponding to peak labelled (A) on the figure. The stronger $\sigma$ hybridisation of the Ti-3*d* $e_g$ orbitals leads to the formation of a broader band and to the corresponding peak (B) on the experimental spectrum. At higher energy, peaks (C) can be attributed to the Ba-5*d* states. As a consequence of the dipole selection rule, the O–K edge probes the O-2*p* projected density of states which extend over this large energy range and then reflects the over all electronic structure of this compound. A direct comparison of these experimental spectra shows important similarities in the number, the energy position and the shape of the different peaks between these two compounds. The main difference comes from the presence of a shoulder labelled (A′) on the low energy side of the first peak in $Ba_3Ti_2MnO_9$. As in the case of the Ti–$L_{23}$ edge, expected changes due to presence of oxygen vacancies, i.e. the over all broadening of the structures lying in the first 10 eV after the edge onset [21,22], are not observed. The (A′) shoulder is absent in $BaTiO_3$ and then appears as a direct consequence of the hybridisation of O-2*p* with Mn-3*d* states, which is consistent with the covalent character of the Mn–O bonding deduced from ligand field multiplets calculations of Mn–$L_{23}$ edge. It can be concluded that the empty 3*d* states of Mn now dominate the bottom of the conduction band. This modification of the O–K edge onset in $d^0$ perovskites arising from the introduction of transition-metal has already been observed in $SrTi_{1-x}Ru_xO_3$ [31]. In this system, a similar pre-edge peak related to the Ru-4*d* empty states appears as a characteristic modification of the O–K edge when increasing the Ru content.

## 4. Discussion

In order to analyse this specific effect, we used the theoretical results published by Moretti and Michel-Calendini [32,33] concerning the impurity energy levels and the stability of transition metal ions in cubic $BaTiO_3$. The molecular-orbital model has been widely used to discuss near-edge fine structure and provides useful information to interpret the O–K edge in transition metal oxides [34,35]. Even if the physics of $Ba_3Ti_2MnO_9$ is far from the picture of Mn impurities in $BaTiO_3$, we can at least discuss these results on a qualitative basis. These authors used the self-consistent-field spin-unrestricted $X\alpha$ method to calculate the electronic structure of substitutional manganese ions with different valence states in $BaTiO_3$ and provided the energy levels of the transition metal 3*d* states with respect to the valence and conduction bands. The valence and conduction bands edges have been extracted from a previous calculation [36] performed for a $TiO_6^{-8}$ cluster. The top of the valence band corresponds to the higher occupied molecular orbital (O-2*p* $t_{1g}$) and is referred as the zero energy because of its pure oxygen character while the bottom of the conduction band corresponds to the lowest Ti-3*d* empty state ($t_{2g}$). This procedure gives rise to a optical band gap of 3.48 eV (from their ground-state calculations) which slightly overestimates the experimental value of 3.2 eV in $BaTiO_3$. The calculations have been performed in $MnO_6^{-12+n}$ clusters (where *n* is the formal valency of the transition metal ion) with an $O_h$ point group and using a unit cell parameter of 0.4 nm, representative of $BaTiO_3$. First of all, the theoretical ground-state of $Mn^{4+}$ predicted with this method corresponds to the high-spin $^4A_2$ symmetry, as found from our multiplets calculations of Mn–$L_{23}$ edge. The energy position of the Mn-3*d* antibonding states are given in Table 2. The filled $2t_{2g}\uparrow$ states are located at the top the valence band whereas both $2t_{2g}\downarrow$ and $3e_g\uparrow$ empty states are lying in the band gap, close to the bottom of the conduction band. Finally, the $3e_g\downarrow$ are found at higher energy, in the conduction band. In light of these results, the shoulder (A′) observed at the O–K edge onset in $Ba_3Ti_2MnO_9$ can be assigned to transitions to $2t_{2g}\downarrow$ and $3e_g\uparrow$ empty states located just below the conduction band, in the band gap of $BaTiO_3$ and form the bottom of the conduction band in $Ba_3Ti_2MnO_9$. Even if these states have a dominant Mn-3*d* character, a non-negligible O-2*p* contribution is then detected at the O–K edge onset. These results are summarized in Fig. 4. The values of exchange and ligand field splitting being relatively close, these two

Table 2
Theoretical energy levels of the 3*d* states of a $Mn^{4+}$ impurity in $BaTiO_3$ from [32]

| Level | $2t_{2g}\uparrow$ | $3e_g\uparrow$ | $2t_{2g}\downarrow$ | $3e_g\downarrow$ | CB |
|---|---|---|---|---|---|
| Energy (eV) | −0.16 | 2.36 | 3.02 | 4.72 | 3.48 |

The energy position is given with respect to the top of the valence band. The position of the conduction band is taken from a similar calculation performed in a $TiO_6^{-8}$ cluster [36].

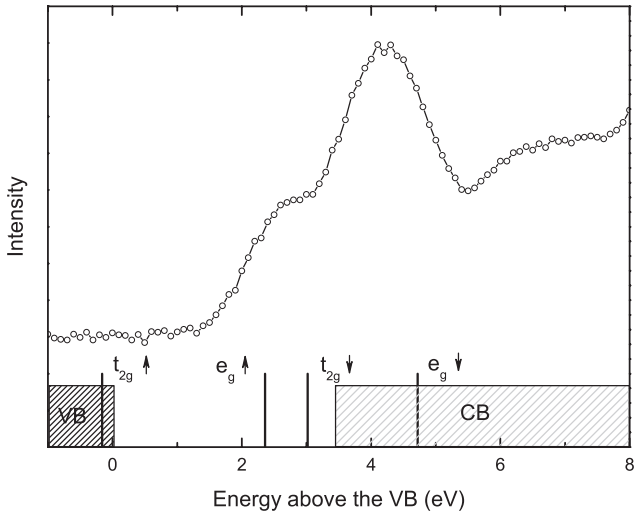


Fig. 4. Schematic representation of a Mn impurity 3*d* levels with respect to the valence (VB) and conduction (CB) bands of cubic $BaTiO_3$ from [32] compared to the O–K edge onset in $Ba_3Ti_2MnO_9$.

states correspond to similar energy positions (separated by only 0.66 eV) and as a consequence, only one peak appears on the experimental spectrum. This effect has already been pointed out by de Groot et al. [34] in their study of O–K edge in $Cr_2O_3$ and $MnO_2$. Another possible reason for this discrepancy comes from the energy spread of these states due to the bond formation in the solid, leading to an over all broadening of these peaks. In other words, the Mn cannot be considered as an impurity in $Ba_3Ti_2MnO_9$. Finally, the 1*s* core-hole left by the excited electron should lead to a modification of this ground-state electronic structure. The high-lying $3e_g \downarrow$ states fall in an energy range dominated by the empty Ti-3*d* states. It is not possible to identify any specific features related to these states in the experimental spectrum. Finally, from the population analysis, the authors emphasized the covalent character of the Mn–O bonding clearly observed in our experiments on both O–K and Mn–$L_{23}$ edges.

## 5. Conclusion

Important information has been extracted from the analysis of the near-edge fine structure observed in $Ba_3Ti_2MnO_9$. First of all, the Mn–$L_{23}$ edge is characteristic of $Mn^{4+}$ in octahedral crystal field both because of its similarities with well-known signatures of $Mn^{4+}$ found in the literature and because of the good agreement obtained with atomic multiplets calculations. Its $^4A_2$ symmetry is also coherent with the ground-state found from molecular-orbital calculations of $Mn^{4+}$ impurity in cubic $BaTiO_3$. However, the strong reduction of electron–electron interactions needed to get this good agreement suggests that an important hybridisation takes place between the transition metal and the ligand O atoms. This effect is confirmed by the presence of an extra shoulder on the low energy side of the first preeminent peak of the O–K edge, then indicating a Mn-*d* dominant character at the bottom of the conduction band. This shoulder has been attributed to transitions to Mn $2t_{2g} \downarrow$ and $3e_g \uparrow$ empty states, predicted from the same molecular orbital calculations, to be located in the $BaTiO_3$ band gap, close to the bottom of the conduction band. Finally, the analysis of the Ti–$L_{23}$ edge and its comparison with a reference acquired in $BaTiO_3$ confirms both the presence of $Ti^{4+}$, as expected from the results obtained on the Mn edge and the absence of detectable O vacancies. From these experiments, we cannot conclude to a direct interaction between neighbouring Mn and Ti atoms located in edge shared octahedra but the O site shows interaction from both Mn and Ti. It is still not clear if an interaction through the O sites is at the origin of the stabilisation of the hexagonal structure.

## References


[1] P.E. Batson, Nature 366 (1993) 727.
[2] I. Arslan, N.D. Browning, Phys. Rev. Lett. 91 (2003) 165501.
[3] C. Mitterbauer, G. Kothleitner, W. Grogger, H. Zandbergen, B. Freitag, P. Tiemeijer, F. Hofer, Ultramicroscopy 96 (2003) 469.
[4] S. Lazar, G.A. Botton, M.-Y. Wu, F.D. Tichelaar, H.W. Zandbergen, Ultramicroscopy 96 (2003) 535.
[5] A.T. Paxton, M. van Schilfgaarde, M. MacKenzie, A.J. Craven, J. Phys.: Condens. Matter (2000) 725.
[6] J.G. Dickson, L. Katz, R. Ward, J. Am. Chem. Soc. 83 (1961) 3026.
[7] P.C. Donohue, L. Katz, R. Ward, Inorg. Chem. 5 (1966) 339.
[8] J.B. Goodenough, J.A. Kafalas, J. Solid State Chem. 6 (1973) 493.
[9] N. Takeuchi, S. Ishida, M. Wakamatsu, in: Memoirs of the Faculty of Engineering and Design, 43, Kyoto Institute of Technology, 1995, 51.
[10] A. Kirianov, N. Ozaki, H. Ohsato, N. Kohzu, H. Kishi, Jpn. J. Appl. Phys. 40 (2001) 5619.
[11] I.E. Grey, L.M.D. Cranswick, C. Li, J. Appl. Cryst. 31 (1998) 692.
[12] H.T. Langhammer, T. Muller, A. Polity, K.-H. Felgner, H.-P. Abicht, Mater. Lett. 26 (1996) 205.
[13] F.M.F. de Groot, J.C. Fuggle, B.T. Thole, G.A. Sawatzky, Phys. Rev. B 41 (1990) 928.
[14] F.M.F. de Groot, Coord. Chem. Rev. 31 (2005) 249.
[15] F.M.F. de Groot, J.C. Fuggle, B.T. Thole, G.A. Sawatzky, Phys. Rev. B 42 (1990) 5459.
[16] M. Abbate, F.M.F. de Groot, J.C. Fuggle, A. Fujimori, Y. Tokura, Y. Fujishima, O. Strebel, M. Domke, G. Kaindl, J. van Elp, B.T. Thole, G.A. Sawatzky, M. Sacchi, N. Tsuda, Phys. Rev. B 44 (1991) 5419.
[17] P.F. Schofield, C.M.B. Henderson, G. Cressey, G. van der Laan, J. Synchrotron Radiat. 2 (1995) 93.
[18] F.M.F. de Groot, M.O. Figueiredo, M.J. Basto, M. Abbate, H. Petersen, J.C. Fuggle, Phys. Chem. Miner. 19 (1992) 140.
[19] K. Okada, A. Kotani, J. Electron Spectrosc. Relat. Phenom. 62 (1993) 131.
[20] G. van der Laan, Phys. Rev. B 41 (1990) 12366.
[21] G.Y. Yang, E.C. Dickey, C.A. Randall, M.S. Randall, L.A. Mann, J. Appl. Phys. 94 (2004) 5990.
[22] D.A. Muller, N. Nakagawa, A. Ohtomo, J.L. Grazul, H.Y. Hwang, Nature 430 (2004) 657.
[23] F.M.F. de Groot, Ph.D. Thesis, University of Nijmegen, 1991.
[24] R. Moroni, Ch. Cartier dit Moulin, G. Champion, M.-A. Arrio, Ph. Sainctavit, M. Verdaguer, D. Gatteschi, Phys. Rev. B 68 (2003) 064407.
[25] F.M.F. de Groot, J. Electron Spectrosc. Relat. Phenom. 67 (1994) 529.
[26] B. Gilbert, B.H. Frazer, A. Belz, P.G. Conrad, K.H. Nealson, D. Haskel, J.C. Lang, G. Srajer, G. De Stasio, J. Phys. Chem. A 107 (2003) 2839.
[27] L.A.J. Garvie, A.J. Craven, R. Brydson, Am. Mineral. 79 (1994) 411.
[28] C. Elsasser, S. Kostlmeier, Ultramicroscopy 86 (2001) 325.
[29] F.M.F. de Groot, J. Faber, J.J.M. Michiels, M.T. Czyzyk, M. Abbate, J.C. Fuggle, Phys. Rev. B 48 (1993) 2074.
[30] G. Radtke, G.A. Botton, submitted for publication.
[31] M. Abbate, J.A. Guevara, S.L. Cuffini, Y.P. Mascarenhas, E. Morikawa, Eur. Phys. J. B 25 (2002) 203.
[32] P. Moretti, F.M. Michel-Calendini, Phys. Rev. B 34 (1986) 8538.
[33] P. Moretti, F.M. Michel-Calendini, Phys. Rev. B 36 (1987) 3522.
[34] F.M.F. de Groot, M. Grioni, J.C. Fuggle, J. Ghijsen, G.A. Sawatzky, H. Petersen, Phys. Rev. B 40 (1989) 5715.
[35] H. Kurata, C. Colliex, Phys. Rev. B 48 (1993) 2102.
[36] F.M. Michel-Calendini, H. Chermette, J. Weber, J. Phys. C: Solid State Phys. 13 (1980) 1427.